Lab on a Chip

PAPER

View Article Online
View Journal | View Issue

Cite this: *Lab Chip*, 2022, **22**, 2192

Semi-automated preparation of fine-needle aspiration samples for rapid on-site evaluation†

Filipe Marques, [a] Janosch Hauser, [a] Emre Iseri, [a] Igor Schliemann,[b] Wouter van der Wijngaart[a] and Niclas Roxhed*[ac]

Received 14th March 2022,
Accepted 6th May 2022

DOI: 10.1039/d2lc00241h

rsc.li/loc

Rapid on-site evaluation (ROSE) significantly improves the diagnostic yield of fine needle aspiration (FNA) samples but critically depends on the skills and availability of cytopathologists. Here, we introduce a portable device for semi-automated sample preparation for ROSE. In a single platform, the device combines a smearing tool and a capillary-driven chamber for staining FNA samples. Using a human pancreatic cancer cell line (PANC-1) and liver, lymph node, and thyroid FNA model samples, we demonstrate the capability of the device to prepare samples for ROSE. By minimizing the equipment needed in the operating room, the device may simplify the performance of FNA sample preparation and lead to a wider implementation of ROSE.

Introduction

Endoscopic ultrasound-guided fine needle aspiration (EUS-FNA) is a needle biopsy technique that allows minimally-invasive sampling of potentially malign tumors in deep-seated organs.[1] Rapid on-site evaluation (ROSE) is a real-time service during EUS-FNA interventions, that assesses the adequacy of the collected biopsy samples for diagnostics. Sample adequacy is deemed by the number of target cells that allow determining tumor malignancy. ROSE reduces the overall number of needle passes required for an appropriate sample and the number of FNA procedures.[2] ROSE is typically performed in the operating room and starts by transferring an aliquot of the FNA sample onto a glass slide. Then, the sample is manually smeared out to obtain a thin sample layer with cells dispersed along the glass slide. After an air-drying step, the sample is stained, typically with a rapid Romanowky-type stain. Finally, a morphological assessment of the stained cells under a microscope allows to evaluate the adequacy of the collected FNA sample.[3] Depending on the medical procedure, FNA sample properties, such as viscosity, vary widely between patients and between source organs.[4–6] Samples may also present tissue fragments or clots requiring further processing or analytical methods.[7] Therefore, performing the sample preparation for ROSE requires expertise and is typically carried out by trained personnel, *e.g.*, cytopathologists. However, health centers are often reluctant to perform ROSE due to the limited time or lack of cytopathologists.[2,8] To address these challenges, new alternatives methods using telecytopathology and artificial intelligence (AI) have been investigated. However, both methods require trained personnel on-site to prepare samples.[9,10] Alternatives to replace cytopathologists for ROSE sample preparation include the use of ThinPrep® instruments or alternative evaluators (AE), *i.e.* clinicians, nurses, cytotechnicians, trained to implement ROSE.[11] However, ThinPrep® instruments are too slow to prepare the time-critical samples on-site and AE require up to a year of training and have a diagnostic accuracy ranging from 73.5% to 98% due to a high dependency on the skill of the operator.[11,12]

Here, we present a portable sample preparation device that allows healthcare personnel to perform ROSE of FNA samples. The device consists of a smearing tool and a capillary-driven microfluidic chamber containing a water-soluble film with cell stain, designed to simplify sample preparation for ROSE (Fig. 1). Using the device, we performed ROSE sample preparation of a multitude of FNA model samples with different viscosity and origin, such as pancreatic cells (PANC-1), porcine liver, lymph node, and thyroid samples.

Working principle and device design

The device is designed for single-use and consists of a tool for smearing the FNA sample on a glass slide, connected to a capillary-driven microfluidic chamber for controlled staining of cells (Fig. 1a). The smearing tool is designed as a bird-type film applicator for manual spreading of a liquid sample over a glass

[a] *Division of Micro and Nanosystems, KTH Royal Institute of Technology, 10044 Stockholm, Sweden. E-mail: roxhed@kth.se*
[b] *Pathology and Cytology Department, Karolinska University Hospital, Stockholm, Sweden*
[c] *Medtech Labs, Karolinska hospital, Stockholm, Sweden*

† Electronic supplementary information (ESI) available: Device layout, stain film fabrication, cell culture and FNA viscosity model preparation, robotic stage, microscopy images See DOI: **https://doi.org/10.1039/d2lc00241h**

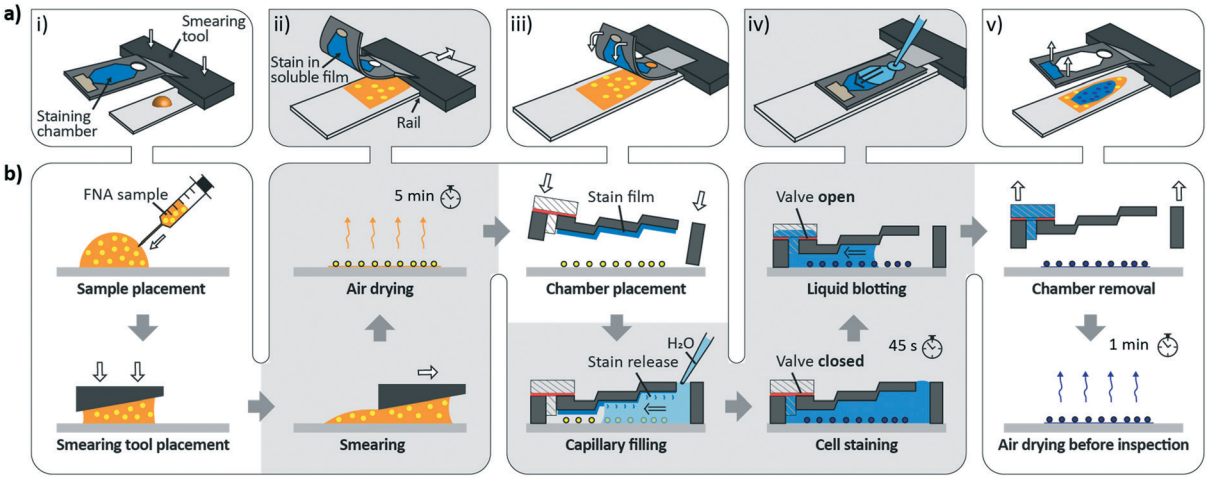

Fig. 1 a) The five device operation steps and b) detailed workflow of the portable microfluidic device for preparing samples for ROSE. i) Place sample aliquot on a glass slide and bring the smearing tool in contact with the sample. ii) Smear the sample and allow to dry in air. iii) Fold the microfluidic staining chamber to cover the smear. iv) Add water, which fills the microfluidic chamber by capillary action and releases the stain from the dry film. Cell staining proceeds until the dissolvable valve opens and the liquid is absorbed by the downstream blotting paper. v) Remove the chamber and allow to air dry before microscopy inspection.

slide, with rails to guide the smearing along the glass slide. The microfluidic staining chamber has a volume of 300 μL and allows cell staining with few and non-critical user interactions. The inner surface of the chamber lid is coated with a soluble stain layer that releases stain into the liquid upon chamber filling with water. A downstream blotting unit contains two blotting papers that are separated from the staining chamber by a water-soluble film. The dissolving time of this film controls the time that the cells are in contact with the stain. The staining chamber connects to the smearing tool with a hinge, which aligns the chamber with the glass slide (Fig. 2).

Sample preparation with the device proceeds with five operation steps (Fig. 1). In step i), the smearing tool is placed onto a 10 μL liquid FNA sample on the glass slide. In step ii), the smearing tool is moved along the glass slide, guided by the rails, thus smearing out the sample into a thin liquid film in a controlled way. During approximately five minutes the liquid film dries upon exposure to air, fixating the cells. In step iii), the microfluidic staining chamber is folded over and attached to the glass slide. In step iv), water is added to the inlet, which results in capillary filling of the staining chamber. During this process, the stain film immediately dissolves, and the fixated cells become stained. Once the water-soluble film is dissolved, the liquid is blotted from the staining chamber, exposing the stained cells to air. In step v), the staining chamber is removed, and the glass slide is left to dry for approximately one minute before being ready for imaging.

Experimental

Materials

Hydrophilic sheets, Xerox type C laser printing transparency were acquired from Elmstock (Wisbech, UK). Adhesive tape 64620 was obtained from Tesa (Norderstedt, Germany). Ahlstrom grade 270 and 601 (Ahlstrom Filtration LLC, Mt. Holly Springs, USA) were used as blotting paper in the blotting unit. Poly(vinyl alcohol) (PVA) 360627 was obtained from Sigma-Aldrich (Stockholm, Sweden). Wright–Giemsa Stain, Modified WG16 was acquired from Sigma-Aldrich (Stockholm, Sweden). Giemsa stain G5637 was acquired from Merck (Stockholm, Sweden). Scotch® permanent double-sided tape 2346832 was purchased from Office Depot (Stockholm, Sweden). Xerox multipurpose paper was acquired from Office Depot (Stockholm, Sweden). Laminating pouches A4 100 μm were acquired from Office Depot (Stockholm, Sweden). Deionized (DI) water had a resistivity of >18 MΩ cm. Dulbecco's Modified Eagle Medium (DMEM) (high glucose) was acquired from Gibco (Gothenburg, Sweden). Fetal bovine serum (FBS) was obtained from Gibco (Gothenburg, Sweden). Penicillin–Streptomycin (PS) was acquired from Gibco (Gothenburg, Sweden). Gibco™ GlutaMAX™ was purchased from Gibco (Gothenburg, Sweden). Absolute ethanol 20820 was obtained from VWR (Stockholm, Sweden). Whatman® Anotop® 10 Plus syringe filters were acquired from Merck (Stockholm, Sweden). White sugar cubes were acquired from Dan Sukker (Stockholm, Sweden). Spec-Wipe® 3 Cleanroom wipers 21912-042 were purchased from VWR (Stockholm, Sweden). Normal Saline 0.9% solution 786 was obtained from VWR (Stockholm, Sweden). DPBS Gibco™ 14190 was purchased from Thermo Fisher Scientific (Stockholm, Sweden). Countess™ cell counting chamber slide C10228 and Trypan Blue 0.4% were acquired from Thermo Fisher Scientific (Stockholm, Sweden). Superfrost® Plus adhesion glass slide 12312148 was acquired from Fisher Scientific (Stockholm, Sweden).

Device fabrication

The device consists of two elements, the smearing tool and the microfluidic staining chamber. The smearing tool was

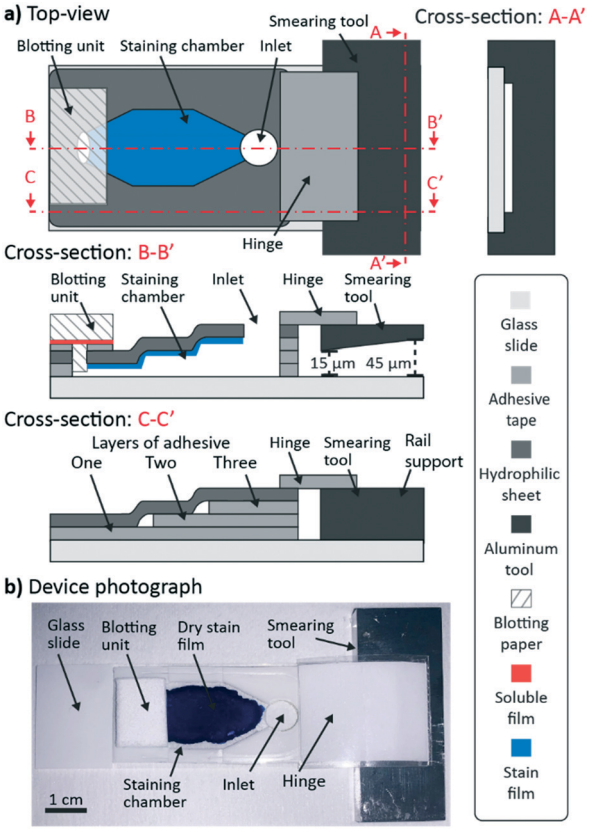

Fig. 2 a) Schematic views of the device. Top view indicating the blotting unit, the staining chamber with an inlet and the smearing tool connected by a hinge. Cross-sectional view along A-A′ showing the smearing tool mounted on the glass slide and the respective smearing area between them. Cross-sectional view along B-B′ showing the blotting unit, consisting of two layers of blotting paper with a soluble film in between, the staining chamber containing the stain film, and the smearing tool connected to the staining chamber by a hinge. Cross-sectional view along C-C′ showing different number of adhesive layers and the smearing tool rail support. b) A photo of a fabricated device with dimensions 9.9 × 5.8 cm^2.

milled from aluminum by computer numerical control (CNC) milling with micrometer precision (MiniMill GX, Minitech Machinery Corp., Norcross, GA, USA) and could be fabricated in plastic as to facilitate disposal. The microfluidic staining chamber was fabricated using lamination technology, as described earlier.[13–15] Three different material layers, as indicated in Fig. 2, were structured using a cutting plotter (CE6000, Graphtec America Inc., Irvine, CA) and assembled using alignment pins. The design of the device layers is detailed in the ESI.† The blotting paper was cut using a laser cutter (VLS 2.30, Universal Laser Systems, Vienna, Austria). The water-soluble film in the blotting unit was fabricated from granular PVA using a thin-film applicator (4340, Elcometer, Manchester, UK), as described in the ESI.† The resulting film thickness was measured with a thickness gauge with 1 µm graduation (2109L Metric Dial Gauge, Mitutoyo, Upplands Väsby, Sweden). The soluble film was laminated to the upper blotting paper at 80 °C using a HeatSeal™ H600 Pro laminator (GBC®, Northbrook, IL, USA).

The stain layer inside the staining chamber consists of Giemsa stain and PVA, fabricated by drop-casting a 300 µL solution and letting it dry overnight inside the chamber. Details of the stain concentration and film fabrication are given in the ESI.† The resulting film thickness was measured with the thickness gauge to be 5 µm. The smearing tool and the microfluidic chamber were combined by a hinge consisting of a 2 cm × 4 cm laminated multipurpose paper with a bottom layer of double-sided tape. Lamination was performed with a Leitz Laminator A3 (Leitz GMBH & Co., Oberkochen, Germany). The hinge was placed on top of the smearing tool and the microfluidic chamber just before the inlet.

Smearing tool use

In preparation for smearing, 10 µL of a sample was gently homogenized with a pipette by aspirating and dispensing liquid in 2 s cycles for 30 s and placed at the proximal end of a glass slide. The smearing tool was placed on top of the sample for 5 s, allowing the sample to fill the space between the tool and the glass slide. Then, the smearing tool was moved from the proximal to the distal end of the glass slide in one steady motion spreading the sample along the glass slide surface. Sample fixation followed by air drying for 5 minutes.

During manual use, sample spread was performed at a speed of approximately 5 cm s^{-1} and the smearing tool was left at the distal end of the glass slide during sample fixation.

Effect of smearing speed and sample viscosity

To assess the effect of smearing speed and sample viscosity during FNA sample spreading, we mounted the smearing tool on a custom-built stage (details in ESI†) and performed cell smears at different speeds and sample viscosities (Fig. 3a and b). The stage allowed to control the stage speed in the range 1–7 cm s^{-1}. We kept the smearing tool stationary while the stage moved underneath with a glass slide. We created a FNA sample model using a human pancreatic cancer cell line PANC-1, as detailed in the SI. The majority of cystic samples present viscosities within 1 mPa s and 10 mPa s, with the possibility of highly viscous samples that cannot be aspirated *via* FNA.[16,17] We used the PANC-1 sample with low (1 mPa s) and medium (57 mPa s) viscosity, obtained by the addition of sugar, as described in the ESI.† The samples, as measured in a Countess II FL automated cell counter (Thermo Fisher Scientific, Sweden), had a concentration of 1.1 × 10^6 cells mL^{-1}.

Smears were prepared as described above. The stage was moved at 1 cm s^{-1}, 3 cm s^{-1}, 5 cm s^{-1} or 7 cm s^{-1} to smear samples. Stage movement was repeated five times per sample and speed setting, resulting in 40 prepared glass slides. Between tests, the smearing tool was rinsed with DI water and scrubbed with cleanroom wipers. Smears were manually stained using Wright–Giemsa stain following the protocol provided by the supplier.

We evaluated the smearing quality and repeatability by manually counting cells in a predefined cell counting area

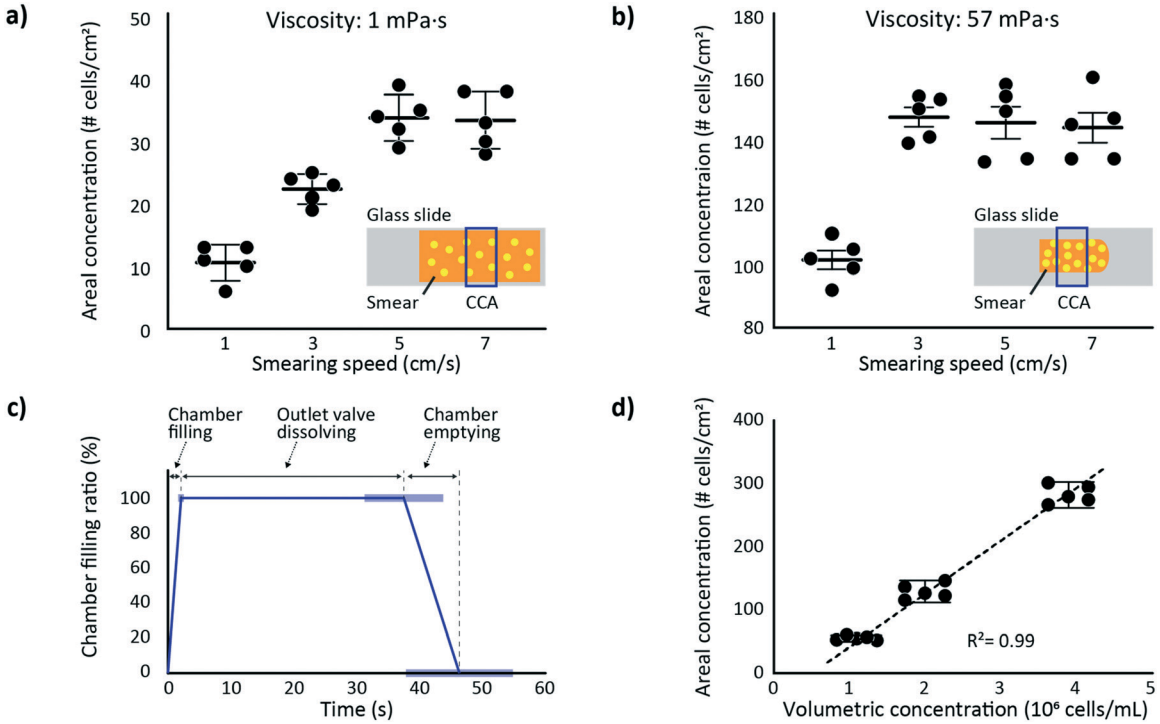

Fig. 3 Measured number of cells per area at different smearing speeds for PANC-1 water-based samples with viscosity a) 1 mPa s and b) 57 mPa s. Smear illustrations exemplify the lateral spread of the sample, at smearing speeds ≥5 cm s^{-1} and ≥3 cm s^{-1} for 1 mPa s and 57 mPa s samples, respectively. The blue box indicates the cell counting area (CCA). c) The chamber filling ratio over time as extracted from video sequences resolves the three stages of the microfluidic staining sequence: chamber filling, outlet valve dissolving and chamber emptying. The plotted data is calculated as an average from six devices and error bars represent standard deviations. d) Areal density of dyed cells after preparation of a low viscosity sample at approximately 5 cm s^{-1} *versus* the cell concentration of the sample and respective linear curve fit (dashed line).

(CCA) on the glass slides. To consistently define the CCA between different glass slides we fabricated a custom-made frame by laser cutting a piece of PMMA with 1 cm × 2 cm defining the CCA. For each of the replicates with the same sample viscosity we placed the frame in the same position. Due to different sizes of the spreading area between the different sample viscosities, the position of the CCA was moved 1 cm towards the proximal end of the glass slide for medium viscosity samples. For the purpose of ROSE, the absolute position of the sample on the glass slide is of less importance than the quality of the spread sample. Glass slides were evaluated using a Zeiss Axio Scope A1 with a 10× (Zeiss, N-Achroplan 10×/0.25, 420941-9910) objective. Only the cells within the CCA were considered and normalized to cells cm^{-2}.

Microfluidic staining sequence

To test the timing consistency of the microfluidic staining sequence we fabricated six staining chambers without stain, added 300 μL of dyed water and took videos of the microfluidic device sequence. The thickness of the water-soluble film in the blotting unit was 24 μm. From the videos we extracted the times for chamber filling, outlet valve dissolving and chamber emptying.

Sample preparation repeatability and linearity

To test the complete sample preparation procedure, we fabricated 15 microfluidic staining chambers containing dry stain films and reutilized the smearing tool following the previous scrubbing method. In this experiment we controlled the staining time manually, by blotting the liquid after 30 s. Following cell concentrations commonly found in FNA samples, PANC-1 cells at three different cell concentrations ($1.2/2.0/3.9 \times 10^6$ cells mL^{-1}) were used as a FNA model.[18] Concentrations of the samples, stained with Trypan Blue 0.4%, were determined with the cell counter.

Five devices per sample concentration were prepared manually using the smearing tool as described earlier. Then, the microfluidic staining chamber was attached to the glass slide and 300 μL of DI water was pipetted into the inlet. After the manual blotting step, the microfluidic chamber was removed, and excess liquid was left to dry for 1 minute. Smearing evaluation was performed by manually counting cells, using the custom-made CCA frame.

Applicability to different cell types

To test the applicability of the device to different cell types we prepared four different FNA sample models. Three of them were generated from porcine *ex vivo* liver, lymph node and thyroid. These organs were retrieved immediately post-

mortem and placed in a 0.9% saline buffer solution during transport for three hours before use. Before testing, each organ was gently washed for 30 s with tap water and placed in a Petri dish. A scalpel was used to perform a 1 cm deep incision followed by whittling of the incised wall with an up and down movement for 30 s. The resulting liquid present on top of the scalpel blade was transferred to a 2 mL Eppendorf tube containing 500 μL of DPBS. Additionally, we used the human pancreatic tumor cell line, PANC-1, as mentioned above. Smearing was performed manually using the smearing tool as described earlier. The staining chamber, aligned *via* the hinge and the smearing tool, was attached to the glass slide carrying the dried sample. The chamber was primed using 300 μL of DI water, which dissolved the dry stain film and stained the cells. After 30 s the liquid was manually blotted with Ahlstrom grade 222 and the chamber was detached from the glass slide. Finally, the prepared samples were imaged using a fluorescent microscope with 5× (Zeiss, EC Plan-Neofluar 5×/0.16, 420330–9901) and 40× (Zeiss, Plan-Neofluar 40×/1.3, Oil DIC, 420462-9900) objectives, and 10× and 20× (Zeiss, Plan-Apochromat 20×/0.8, 420650-9901) objectives.

Sample preparation with tissue fragment

To assess the ability of the device to handle possible tissue fragments we prepared an FNA sample with an imbedded small intestine fragment. The FNA sample was produced following the "Cell Staining Concentration" procedure in the ESI.† The tissue fragment was cut with a scalpel with dimensions 2 × 1 mm^2, cleaned with tap water for 1 min and added to the FNA sample. Then, approximately 10 μL of sample plus tissue fragment were placed in a glass slide and submitted to the device procedure as explained in "Applicability to Different Cell Types" section, apart from the final air-drying step taking 10 minutes.

Results and discussion

Effect of smearing speed and sample viscosity

The smearing tool produced a consistent smear when using smearing speeds ≥5 cm s^{-1} independently of the two viscosities 1 mPa s and 57 mPa s (Fig. 3a and b). Smearing speeds ≤3 cm s^{-1} in low viscosity samples resulted in the accumulation of sample at the distal end of the glass slide and poor cell adhesion. For increasing smearing speed and increasing sample viscosity, the smear size decreased, as reflected in the increasing areal cell density (Fig. 3a and b). While results for the different sample viscosities are not directly comparable due to different location of the CCA, the results show that the smearing tool can handle samples in a realistic viscosity range (1–57 mPa s). In the conventional smearing procedure, an auxiliary glass slide is used to perform the spreading. This auxiliary glass slide needs to be held at a specific angle and moved at a controlled speed, in order to obtain good spreading, making this step highly dependent on the skill of the operator. Compared to the conventional procedure, the presented smearing tool could facilitate the smearing process, where the user is only required to move the smearing tool, guided by rails, at a moderate speed.

Microfluidic staining sequence

The capillary filling of the chamber (2.1 ± 0.4 s, n = 6) and the water-soluble film dissolution time (38 ± 6 s, n = 6) resulted in an overall staining sequence time of 46 ± 8 s (Fig. 3c). The rapid capillary filling ensures a well-defined and reliable start of the staining procedure throughout the chamber, the variation in overall staining time is low. The overall staining time exceeds well the 10 s that we observed is needed for sufficient cell staining. The results demonstrate that the microfluidic staining chamber enables a well-controlled semi-automated cell staining, triggered by a single and non-critical user interaction: water addition to the inlet of the chamber.

Sample preparation repeatability and linearity

We tested Giemsa stain concentrations between 5–20 mg mL^{-1} and found that concentrations above 5 mg mL^{-1} provided sufficient staining of cells (details in ESI†). Hence, the water-soluble film was produced with an initial solution of 15 mg mL^{-1}. We observed a good linear relation between the cell concentration in the sample and the resulting areal density of stained cells (Fig. 3d). A coefficient of determination R^2 = 0.99 shows that the smears prepared by the device reflect the cell concentration of the original sample. This is a crucial feature for a ROSE procedure when assessing the adequacy of an FNA sample, where too few relevant cells require an extra needle pass. Whilst the device requires five operational steps, a maximum CV of 9% indicate that all steps are repeatable and provide repeatable results for cell concentrations between 1.2–3.9 × 10^6 cells mL^{-1}. While this does not imply an increased diagnostic accuracy, these results show that the presented device can prepare FNA samples with cell concentrations in a relevant range, between what is considered by cytopathologysts as low and moderate cellularity scores.[19]

Applicability to different cell types

5× magnification images show a monolayer spread of cells all over the glass slides without particular pattern for all four cell types: pancreatic, lymph node, liver, and thyroid (Fig. 4). 40× magnification images show cell details that are clearly demarked in relation to the background and with clear distinction of cell sizes and shapes. Further microscopy images of the four cell types at 10× and 20× magnification are shown in the ESI.† In Fig. 4D, one can clearly distinguish atypical pancreatic ductal cells, with variations in their respective sizes and shapes clearly indicating malignancy.[20,21] These features show that the device is capable of preparing ROSE smears and stains for samples of different organs and respective analyses.

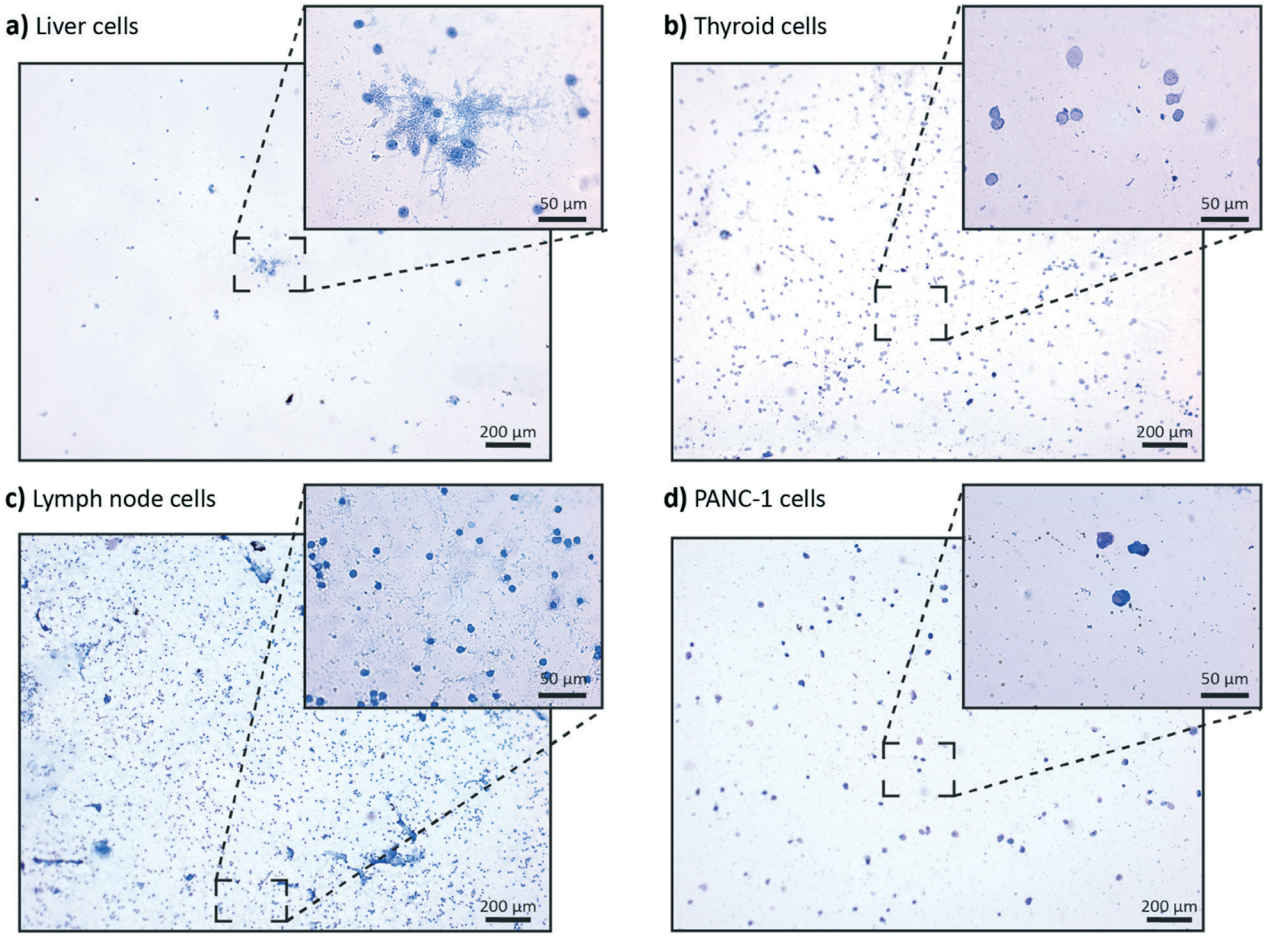

Fig. 4 Contrast enhanced images of different cell types prepared with the ROSE sample preparation device: a) liver cells; b) thyroid cells; c) lymph node cells; d) PANC-1 cells. Individual stained cells are clearly visible as blue dots on a bright background.

Handling of complex samples

The ROSE preparation device showed no adversities staining a tissue fragment of relatively large dimensions, "flattening" the fragment upon smearing and still allowing the passage of water in the microfluidic chamber. 5× and 20× magnification images of the prepared fragment depict uniform staining of the tissue and stained cells, respectively. Microscopy images are shown in the ESI.† The successful staining of this tissue fragment shows that the device can handle such predicaments in real samples, where tissue fragments would be of smaller dimensions as to fit inside the lumen of a FNA needle with a maximum diameter of 0.84 mm (18G needle).[22] However, clotted samples remain a problem in cytology.[23] Similar to the conventional technique, smearing a clot with our device would result in a thick smear, entrapping diagnostic cells and making visualization difficult. Given that the device only uses 10 µL of sample, the majority of the FNA sample (within 0.1–65 mL) could still be used for cell block to process sediments, blood clots or large tissue fragments.[24] Our chosen Giemsa staining procedure is compatible with genetic analysis.[25] Therefore, samples prepared with our device could be further used by scrapping material from the glass slide for ThinPrep® preparation or molecular analysis *via* DNA/RNA extraction, following common procedure.[26]

Conclusions

We successfully tested a portable device designed for healthcare personnel to perform ROSE of FNA samples. We found that the smearing tool presented consistent cell counts at speeds above 5 cm s^{-1}, both for medium and low viscosity samples. We showed the consistency of the microfluidic staining sequence, taking 46 ± 8 s to complete. We showed the repeatability of the full device with a maximum CV of 9% at 1.2, 2, and 3.9 × 10^6 cells mL^{-1} and a linearity with a coefficient of determination R^2 = 0.99. We assessed applicability by using the device on porcine liver, thyroid and lymph node and human PANC-1 cells, showing the ability to detect cells and to assess cell shapes, sizes, background and malignancy. We showed that the device could successfully prepare samples with tissue fragments. The ROSE preparation device proves to be versatile, robust, and a tool with the potential to disseminate ROSE and thereby facilitate an improved yield of FNA. We propose two possible deployment modes for our device. In a first mode, our device

would be used by a nurse or a medical doctor to prepare ROSE, in the operating room to image and analyze the samples. In a second mode, nurses or medical doctors would prepare and image relevant sections of the glass slides using our device and subsequently such images would be analyzed by telecytopathology or AI. Although the device operators require specific training to determine which features are relevant, both approaches could help to provide ROSE where cytopathologists are not readily available.

Author contributions

FM, JH, and NR conceived the original idea. FM, JH, EI, WW, NR designed the device. FM, JH, EI fabricated devices and performed experiments. FM, JH, IS analyzed the data. FM and JH wrote the initial draft. All authors edited or commented on the final version.

Conflicts of interest

There are no conflicts to declare.

Acknowledgements

The research was partially funded by a grant provided by Region Stockholm (HMT project #20180849). We thank Urban Arnelo, Pellina Janson and KERIC for providing porcine organs. We thank Rainer Heuchel and PaCaRes Lab for providing PANC-1 cells. We thank Mikael Bergqvist for CNC milling of the aluminum smearing device.

References

1 P. VanderLaan, Fine-needle aspiration and core needle biopsy: An update on 2 common minimally invasive tissue sampling modalities, *Cancer Cytopathol.*, 2016, **124**(12), 862–870.
2 G. da Cunha Santos, H. Ko, M. Saieg and W. Geddie, "The petals and thorns" of ROSE (rapid on-site evaluation), *Cancer Cytopathol.*, 2012, **121**(1), 4–8.
3 P. Shield, J. Cosier, G. Ellerby, M. Gartrell and D. Papadimos, Rapid on-site evaluation of fine needle aspiration specimens by cytology scientists: a review of 3032 specimens, *Cytopathology.*, 2014, **25**(5), 322–329.
4 P. Eisendrath and M. Ibrahim, How good is fine needle aspiration? What results should you expect?, *Endosc. Ultrasound*, 2014, **3**(1), 3.
5 E. Vazquez-Sequeiros, I. Norton, J. Clain, K. Wang, A. Affi and M. Allen, *et al.*, Impact of EUS-guided fine-needle aspiration on lymph node staging in patients with esophageal carcinoma, *Gastrointest. Endosc.*, 2001, **53**(7), 751–757.
6 S. Alkaade, E. Chahla and M. Levy, Role of endoscopic ultrasound-guided fine-needle aspiration cytology, viscosity, and carcinoembryonic antigen in pancreatic cyst fluid, *Endosc. Ultrasound*, 2015, **4**(4), 299.
7 L. Krogerus and I. Kholová, Cell Block in Cytological Diagnostics: Review of Preparatory Techniques, *Acta Cytol.*, 2018, **62**(4), 237–243.
8 R. Schmidt, B. Walker and M. Cohen, When Is Rapid On-Site Evaluation Cost-Effective for Fine-Needle Aspiration Biopsy?, *PLoS One*, 2015, **10**(8), e0135466.
9 O. Lin, Telecytology for rapid on-site evaluation: current status, *J. Am. Soc. Cytopathol.*, 2018, **7**(1), 1–6.
10 M. Landau and L. Pantanowitz, Artificial intelligence in cytopathology: a review of the literature and overview of commercial landscape, *J. Am. Soc. Cytopathol.*, 2019, **8**(4), 230–241.
11 L. Pearson, R. Factor, S. White, B. Walker, L. Layfield and R. Schmidt, Rapid On-Site Evaluation of Fine-Needle Aspiration by Non-Cytopathologists: A Systematic Review and Meta-Analysis of Diagnostic Accuracy Studies for Adequacy Assessment, *Acta Cytol.*, 2018, **62**(4), 244–252.
12 N. Meena, S. Jeffus, N. Massoll, E. Siegel, S. Korourian and C. Chen, *et al.*, Rapid onsite evaluation: A comparison of cytopathologist and pulmonologist performance, *Cancer Cytopathol.*, 2015, **124**(4), 279–284.
13 J. Hauser, G. Lenk, J. Hansson, O. Beck, G. Stemme and N. Roxhed, High-Yield Passive Plasma Filtration from Human Finger Prick Blood, *Anal. Chem.*, 2018, **90**(22), 13393–13399.
14 J. Hauser, G. Lenk, S. Ullah, O. Beck, G. Stemme and N. Roxhed, An Autonomous Microfluidic Device for Generating Volume-Defined Dried Plasma Spots, *Anal. Chem.*, 2019, **91**(11), 7125–7130.
15 J. Hauser, G. Kylberg, M. Colomb-Delsuc, G. Stemme, I. Sintorn and N. Roxhed, A microfluidic device for TEM sample preparation, *Lab Chip*, 2020, **20**(22), 4186–4193.
16 I. Khamaysi, G. Vasilyev, Y. Chowers and E. Zussman, Su1278 Rheological Analysis of Pancreatic Cyst Fluid Accurately Differentiates Pancreatic Cyst Types, *Gastrointestinal Endoscopy*, 2016, **83**(5), AB333–AB334.
17 L. Walsh, L. Mitchell, A. Johri, N. Matone, M. Frecker and M. Moyer, When high viscosity of pancreatic cysts precludes effective EUS-FNA: a benchtop comparison of negative pressure devices, *Endosc. Int. Open*, 2019, **07**(04), E594–E599.
18 M. Rajer and M. Kmet, Quantitative analysis of fine needle aspiration biopsy samples, *Radiol. Oncol.*, 2005, **39**(4), 269–272.
19 S. Roy-Chowdhuri, H. Chen, R. Singh, S. Krishnamurthy, K. Patel and M. Routbort, *et al.*, Concurrent fine needle aspirations and core needle biopsies: a comparative study of substrates for next-generation sequencing in solid organ malignancies, *Mod. Pathol.*, 2017, **30**(4), 499–508.
20 P. Marchetti, M. Bugliani, V. De Tata, M. Suleiman and L. Marselli, Pancreatic Beta Cell Identity in Humans and the Role of Type 2 Diabetes, *Front. Cell Dev. Biol.*, 2017, **5**, 55.
21 H. Nia, L. Munn and R. Jain, Physical traits of cancer, *Science*, 2020, **370**, 6516.
22 P. VanderLaan, Fine-needle aspiration and core needle biopsy: An update on 2 common minimally invasive tissue sampling modalities, *Cancer Cytopathol.*, 2016, **124**(12), 862–870.
23 C. Michael and B. Davidson, Pre-analytical issues in effusion cytology, *Pleura Peritoneum.*, 2016, **1**(1), 45–56.

24 R. Wardeh, J. Lee and M. Gu, Endoscopic ultrasound-guided paracentesis of ascitic fluid, *Cancer Cytopathol.*, 2010, **119**(1), 27–36.
25 L. Sorber, B. Claes, K. Zwaenepoel, B. Van Dorst, K. De Winne and E. Fransen, *et al.*, Evaluation of Cytologic Sample Preparations for Compatibility With Nucleic Acid Analysis, *Am. J. Clin. Pathol.*, 2021, **157**(2), 293–304.
26 V. Shidham, CellBlockistry: Chemistry and art of cell-block making – A detailed review of various historical options with recent advances, *CytoJournal.*, 2019, **16**, 12.